The American Journal of Pathology, Vol. 179, No. 5, November 2011

DOI: 10.1016/j.ajpath.2011.08.004

Immunopathology and Infectious Diseases

Ineffective CD8$^+$ T-Cell Immunity to Adeno-Associated Virus Can Result in Prolonged Liver Injury and Fibrogenesis

Jessica Spahn,*† Robert H. Pierce,‡ and Ian N. Crispe*†

From the David H. Smith Center for Vaccine Biology and Immunology, University of Rochester Medical Center, Rochester, New York; Seattle BioMedical Research Institute,† Seattle, Washington; and the Department of Pathology,‡ Merck Research Laboratories, Palo Alto, California*

Chronic viral hepatitis depends on the inability of the T-cell immune response to eradicate antigen. This results in a sustained immune response accompanied by tissue injury and fibrogenesis. We have created a mouse model that reproduces these effects, based on the response of CD8$^+$ T cells to hepatocellular antigen delivered by an adeno-associated virus (AAV) vector. Ten thousand antigen-specific CD8$^+$ T cells undergo slow expansion in the liver and can precipitate a subacute inflammatory hepatitis with stellate cell activation and fibrosis. Over time, antigen-specific CD8$^+$ T cells show signs of exhaustion, including high expression of PD-1, and eventually both inflammation and fibrosis resolve. This model allows the investigation of both chronic liver immunopathology and its resolution. ***(Am J Pathol 2011, 179:2370–2381; DOI: 10.1016/j.ajpath.2011.08.004)***

The liver has unique immunological properties that often complicate the ability of the immune system to effectively eliminate hepatotropic pathogens such as hepatitis B and hepatitis C viruses (HBV and HCV). A significant percentage of people infected with these viruses generate ineffective CD8$^+$ T-cell responses that fail to eliminate the pathogen but are capable of causing prolonged liver damage, often resulting in fibrosis, cirrhosis, and hepatocellular carcinoma. For the development of more effective therapies, it is necessary to understand the mechanism by which CD8$^+$ T cells are activated and the reasons for their failure.

The CD8$^+$ T-cell response to hepatocellular-derived antigen is an area of active research. Several studies have shown that hepatocytes are capable of directly activating CD8$^+$ T cells.[1–4] This is unusual, in that primary activation of T cells generally occurs in the lymph node by professional antigen-presenting cells. CD8$^+$ T-cell activation on hepatocytes, however, does not always generate effective immune responses and can even cause the T cells to undergo apoptosis.[3] Hepatocyte-driven activation of CD8$^+$ T cells also leads to the generation of a unique population of PD-1^{hi} cells.[4] These two outcomes, together with poor activation of CD4$^+$ T cells,[4] likely contribute to the tolerogenic environment in the liver and the propensity of hepatotropic pathogens to cause chronic infections and long-term hepatitis.

Many mouse models devised to study hepatitis cause only acute liver damage. The bile duct ligation model does result in chronic injury, but it is less relevant to the immunopathology of viral hepatitis because it is not initiated by a T-cell response. Nonetheless, valuable information has been obtained from these models. The concanavalin A and lipopolysaccharide models have demonstrated the importance of cytokines such as tumor necrosis factor α (TNFα) and interferon γ (IFNγ) in causing liver damage.[5,6] The HBV transgenic model has shown the ability of these cytokines to also control infection in a noncytopathic manner,[7] and the lymphocytic choriomeningitis virus model has described a hepatotropic virus that is eliminated by an effective CD8$^+$ T-cell response.[8]

We have previously used an adeno-associated virus (AAV) model of hepatocellular antigen delivery to study the resulting CD8$^+$ T-cell response. The delivery of a transgene to the liver using AAV as a vector leads to hepatocyte-restricted expression.[9] Approximately 2% to 5% of hepatocytes are transduced with these AAV vectors.[10] Because patients with HCV typically have 5% (but sometimes up to 60%) infected hepatocytes,[11] the num-

Supported by NIH grant DK075274 (I.N.C.).

Accepted for publication August 1, 2011.

Supplemental material for this article can be found at *http://ajp.amjpathol.org* or at doi: 10.1016/j.ajpath.2011.08.004.

Address reprint requests to Jessica Spahn, Ph.D., Department of Surgery, Campus Box 8234-3308 CSRB, 660 S. Euclid Ave., St. Louis, MO 63110. E-mail: spahnj@wudosis.wustl.edu.

ber of antigen-expressing hepatocytes obtained using this vector is analogous to the number infected by HCV. In an AAV study of acute hepatitis, the administration of transgene-specific $CD8^+$ T cells resulted in liver damage that is mediated by both IFNγ and TNFα.[12] $CD8^+$ T cells activated in this manner express a high level of the inhibitory receptor PD-1, but they are also capable of cytotoxicity against antigen-expressing splenocytes.[4,9] When an AAV-OVA vector is used (expressing the whole ovalbumin protein), activation of the $CD8^+$ T cells occurs in a $CD4^+$ T-cell help-independent manner. $CD4^+$ T cells specific for ovalbumin peptides are not activated in this model, based on the absence of carboxyfluorescein succinimidyl ester (CFSE) dilution, down-regulation of CD62L, and up-regulation of CD44. Furthermore, in mice lacking $CD4^+$ T cells, OT-1 $CD8^+$ T cells are activated and proliferate to the same extent as when $CD4^+$ T cells are present.[4]

These experimental models share some features with chronic viral hepatitis, but the injury is acute and self-limiting. To create chronic immunopathology against the same persistent antigen, we used an adoptive transfer of antigen-specific $CD8^+$ T cells at a cell dose much closer to the natural precursor frequency. With the present study, we show that the activation of 1×10^4 OT-1 $CD8^+$ T cells against hepatocyte-derived antigen results in slower clonal expansion, which can be accompanied by long-term inflammation, liver damage, and fibrosis. This immunopathology mimics HCV in many respects, including chronicity, hepatocellular injury, and fibrogenesis. In addition, the strength of the T-cell response dictates the ability of those cells to eliminate vector expression, directly affecting hepatitis.

Materials and Methods

Mice

C57BL/6, B6.SJL-*Ptprc*^{a}*Pepc*^{b}/BoyJ (CD45.1 transgenic), B6.PL-*Thy1*^{a}/CyJ (Thy1.1 transgenic), and C57BL/6J-*Tyr*$^{c\text{-}2J}$/(B6 albino) male mice were purchased from the Jackson Laboratory (Bar Harbor, ME). OT-1 transgenic mice,[13] whose T cells recognize the SIINFEKL peptide, on either the CD45.1 or Thy1.1 background were maintained in house. All animals receiving the AAV-eGFP or AAV-eGFP-SIINFEKL vector were C57BL/6 males between 6 and 7 weeks old. All experiments were approved by the Institutional Animal Care and Use Committee.

AAV Vectors

AAV2 vectors containing either enhanced green fluorescent protein (eGFP) or eGFP-SIINFEKL fusion protein under the control of the human elongation factor α (EF1α) promoter were purchased from the Viral Vector Core Facility of the Columbus Children's Research Institute (Columbus, OH).

Intrahepatic Injection

Mice aged 7 to 8 weeks were anesthetized with tribromoethanol (Avertin; Sigma-Aldrich, St. Louis, MO) at a dose of 0.017 mL/g body weight. A small incision was made just below the sternum, and the right lobe of the liver was exposed. Using a 29G insulin syringe, 60 μL of vector (5.88×10^{10} DNase-resistant particles) was injected directly into the liver. The peritoneal cavity was sutured using absorbable sutures (Vicryl; Ethicon, Somerville, NJ), and the skin was closed with wound clips.

OT-1 $CD8^+$ T-Cell Purification and Adoptive Transfer

$CD8^+$ T cells were isolated from the spleens and lymph nodes of OT-1 transgenic mice. Organs were homogenized between the frosty sides of two slides. After a washing, the cell suspension was layered on top of Lympholyte M density gradient separation medium (Cedarlane Laboratories, Burlington, ON, Canada) and spun at $650 \times g$ for 20 minutes at room temperature. The interface was then collected and counted. The $CD8a^+$ T-cell isolation kit for isolation of untouched $CD8^+$ T Cells was used to purify OT-1 cells resulting in more than 90% purity (Miltenyi Biotec, Auburn, CA; Bergisch Gladbach, Germany). Cells were then labeled with CFSE dye (Invitrogen, Carlsbad, CA) and adoptively transferred into mice through the tail vein in a volume of 200 μL at 3 weeks after AAV injection. These cells were detected by flow cytometry using the allotypic marker CD45.1 after gating on $CD8^+$ T cells.

Bioluminescence Imaging

Mice were anesthetized using ketamine and xylazine (100 mg/kg ketamine; 10 mg/kg xylazine) and then were given an intraperitoneal injection of the substrate, D-luciferin (214 μg/g body weight; Xenogen Biosciences-Caliper Life Sciences, Alameda, CA). After 5 minutes, mice were placed in the imaging chamber of the Xenogen *in vivo* imaging system (IVIS-100). A grayscale image of the mouse was captured with a 10-cm field of view, a 0.2-second exposure time, an f/16 aperture, and an open filter. Bioluminescence data were then acquired with mice positioned supine, to image the ventral surface. Acquisition time was 5 minutes.

Measurement of Serum Aminotransferases

Blood was collected via cardiac puncture and allowed to coagulate at room temperature for 2 to 3 hours. Coagulated blood was then centrifuged and the serum was collected. Samples were sent to the Strong Health Clinical Laboratories (Rochester, NY) or Phoenix Central Laboratory (Everett, WA) for measurement of alanine transaminase (ALT, U/L).

Liver Lymphocyte Isolation

Experimental animals were sacrificed using CO_2, and PBS was injected into the portal vein to flush out peripheral lymphocytes from the liver. Livers were then manually homogenized through a tea strainer using a 5-mL syringe

plunger. The cell suspension was then digested in RPMI 1640 medium containing 0.05% collagenase IV (Sigma-Aldrich) and 0.002% DNase I (Sigma-Aldrich) at 37°C for 40 minutes with gentle agitation. After digestion and washing, the cell pellet was resuspended in 2.75 mL 40% OptiPrep cell separation medium (Accurate Chemical & Scientific Corporation, Westbury, NY) and overlaid with 2.25 mL of serum-free RPMI 1640 medium. The gradient was spun at 1015 × *g* for 25 minutes at 4°C. The interface was collected and stained for flow cytometry.

Flow Cytometry

Cell surface staining was performed using PBS and 1% bovine serum albumin (Sigma-Aldrich). The following antibodies were used: CD8 (53–6.7), CD45.1 (A20), Thy1.1 (OX-7), CD44 (IM7), PD-1 (RMP1-30), CD127 (A7R34), DR5 (MD5-1), and CD62L (MEL-14). Antibodies were purchased from eBioscience (San Diego, CA), BD Biosciences (San Jose, CA), or BioLegend (San Diego, CA). Streptavidin in Pacific Orange was purchased from Invitrogen. Flow cytometric analysis was performed on either a FACSCalibur or LSR II system (BD Biosciences). Data were analyzed using FlowJo software version 6.4.7 (Tree Star, Ashland, OR).

Real-Time PCR

Whole livers were homogenized using a mortar and pestle and liquid nitrogen. RNA was isolated using TRIzol reagent (Invitrogen) according to manufacturer's instructions. Genomic DNA was isolated using phenol-chloroform (Sigma-Aldrich). Custom primers and TaqMan MGB probes for eGFP were designed by Applied Biosystems (Carlsbad, CA). The sequences for the primers and probes were as follows: 5′-GCTACCCCGACCACATGAAG-3′ (forward primer), 5′CGGGCATGGCGGACTT-3′ (reverse primer) and 5′CAGCACGACTTCTTC-3′ (probe). Primer and probe assays were also purchased from Applied Biosystems for CXCL9, CXCL10, ICAM-1, and VCAM-1. For cDNA synthesis, an Applied Biosystems high-capacity cDNA reverse transcription kit was used. PCR reactions were performed using Applied Biosystems TaqMan universal PCR master mix, no AmpErase UNG. All results for real-time quantitative PCR (qPCR) were normalized to β-actin, using an intronic actin sequence for genomic DNA. For quantitative reverse transcription PCR (qRT-PCR), results were normalized to β-actin using an exonic actin sequence. Reverse transcription reactions were performed at the Functional Genomic Center, University of Rochester, as was qPCR using an Applied Biosystems 7900HT sequence detection system; alternatively, these reactions were performed at Seattle Biomedical Research Institute on an Applied Biosystems 7500Fast. Data were analyzed by the ΔCt method, as $2^{-(\text{GFP Mean Ct} - \text{Actin Mean Ct})}$.

Immunohistochemistry

The University of Rochester Medical Center Department of Pathology and Laboratory Medicine or Merck Research Laboratories (Palo Alto, CA) was given formalin-fixed slices of liver tissue after harvest. Tissue was then embedded into paraffin blocks. To detect the presence of hepatitis, H&E staining was performed. Sirius Red was used to demonstrate fibrosis.

Formalin-fixed, paraffin-embedded tissue blocks were also stained for CD3, F4/80, and α-smooth muscle actin (SMA). The CD3 antibody (DakoCytomation, Glostrup, Denmark; Carpinteria, CA) was polyclonal and used at a dilution of 1:200 or 0.6 μg/mL. The F4/80 antibody (eBioscience) was used at 1:400 or 0.5 μg/mL. The anti-SMA antibody (DakoCytomation) was used at a 1:150 dilution.

Statistical Analysis

Data were analyzed using Prism software version 5 (GraphPad Software, La Jolla, CA). Most experiments were analyzed using a Mann-Whitney test, and data are reported as means ± SEM. When indicated, experiments were pooled and analyzed using two-way analysis of variance. Significance was determined by a P value of <0.05.

Results

Adoptively Transferred OT-1 CD8$^+$ T Cells Remain in the Liver Long-Term

To study CD8$^+$ T-cell activation and the associated immunopathology in the liver, an adeno-associated virus-based replication-defective vector was used to deliver a fusion protein of enhanced green fluorescent protein and the ovalbumin peptide SIINFEKL (AAV-GFP-SIINFEKL). By directly injecting this vector into the liver, hepatocyte-restricted expression is achieved.[9] At 3 weeks after vector transduction, OT-1 T cells from a transgenic mouse line whose CD8$^+$ T cells specifically recognize the SIINFEKL peptide in the context of the H-2k^b molecule were adoptively transferred into the host. AAV-GFP-SIINFEKL-treated mice without OT-1 CD8$^+$ T cells were used as controls.

In previous studies, 5 × 10^6 OT-1 T cells were administered, cell numbers peaked at day 3 and contracted thereafter, and this resulted in acute liver damage; however, this injury rapidly resolved, rendering this a limited model for the analysis of chronic liver immunopathology.[12] Badovinac et al[14] have shown that the number of adoptively transferred transgenic cells has a significant influence on the outcome of the CD8$^+$ T-cell response, affecting the proliferative potential, the kinetics of expansion, and the phenotype of the T cells. To gain a better understanding of chronic liver inflammation and to more closely mimic the number of endogenous CD8$^+$ T-cell precursors, we induced liver immunopathology using 1 × 10^4 OT-1 CD8$^+$ T cells. To determine the kinetics of OT-1 CD8$^+$ T-cell expansion using this number of cells, we used OT-1 T cells that express firefly luciferase under control of the human CD2 promoter. These T cells, after administration of the substrate luciferin, produce bioluminescence in the presence of ATP. Using live whole-mouse imaging with a Xenogen IVIS instrument, we were able to obtain longitudinal data showing OT-1 CD8$^+$

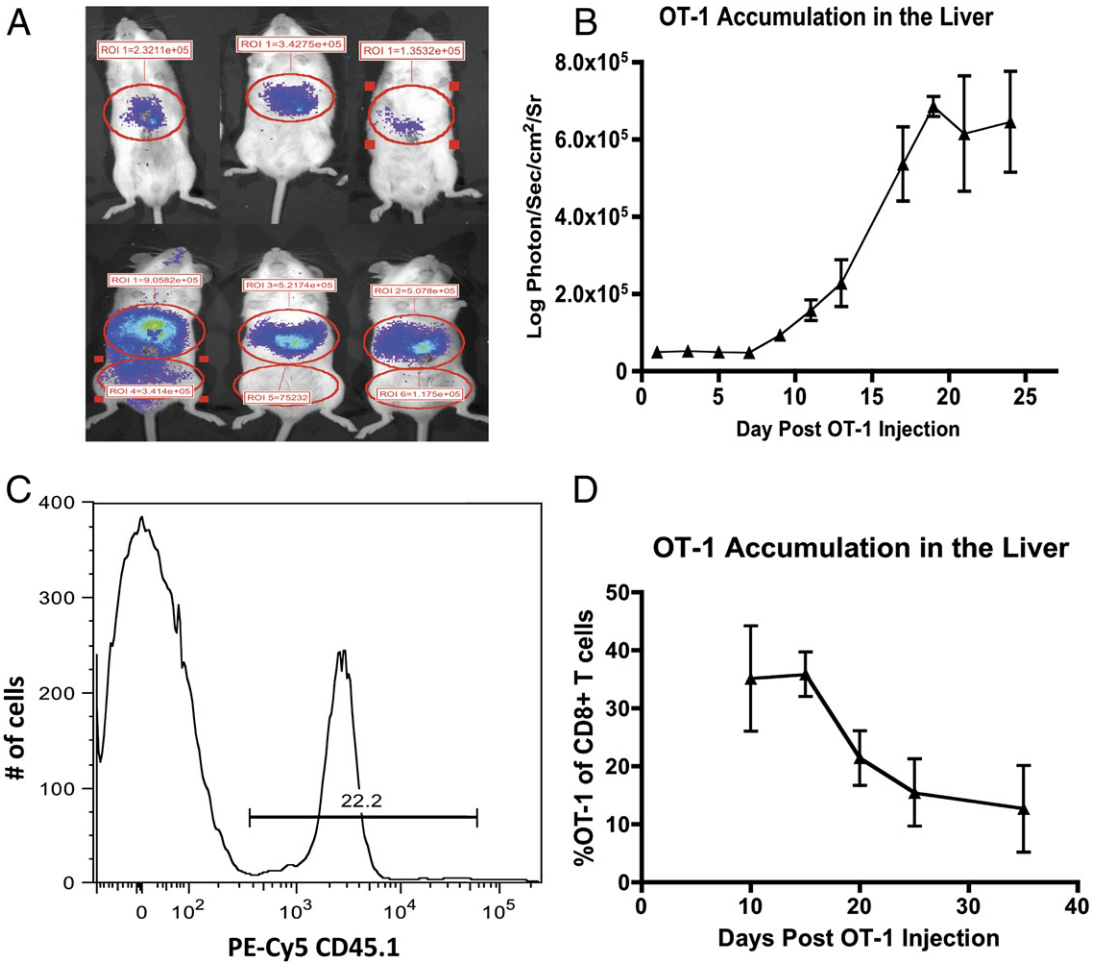

Figure 1. OT-1 CD8$^+$ T cells remain in liver for several weeks after adoptive transfer. C57BL/6-albino (**A** and **B**) or C57BL/6 (**C** and **D**) mice were injected with AAV-GFP-SIINFEKL, followed by 1×10^4 luciferase OT-1 CD8$^+$ T cells (**A** and **B**) or wild-type OT-1 CD8$^+$ T cells (**C** and **D**). **A:** Raw data of live imaging on day 13 (**top row**) and day 23 (**bottom row**). **B:** Graphical representation of live imaging data over a period of 24 days. **C:** Histograms of flow cytometry on day 15. **D:** Graphical representation of flow cytometry data collected every 5 days from day 10 to day 35. $n = 3$, representative of three separate experiments (**A** and **B**); $n = 4$ or 5, representative of two separate experiments (**C** and **D**).

T-cell accumulation in various anatomical sites. The OT-1 CD8$^+$ T-cell localization data are collected in the form of photons emitted in a given area, and this measure is directly correlated with the number of OT-1 CD8$^+$ T cells in a tissue.[15] Representative images for this type of data are shown in Figure 1A. Detection of the OT-1 CD8$^+$ T cells was first seen on day 13 in the area corresponding to the liver, and 10 days later a large expansion of these cells had occurred. This was seen most drastically in one mouse (Figure 1A, bottom left); although in this mouse there is some bioluminescent signal in the lower abdomen, the vast majority of light is being emitted from the area corresponding to the liver. OT-1 CD8$^+$ T cells reached a peak number at approximately day 15, but remained elevated for at least 1 week thereafter (Figure 1B). The bioluminescent signal was significantly stronger than the control level at all points after day 13 ($P < 0.05$).

To confirm these findings, mice were harvested every 5 days after adoptive transfer from day 10 to day 35. Flow cytometry was used to detect the OT-1 CD8$^+$ T cells by gating on CD8$^+$ T cells and the allotypic marker CD45.1. This alternative method corroborated the previous findings obtained using live imaging (Figure 1, C and D). A peak in OT-1 CD8$^+$ T-cell frequency was reached between days 10 and 15, after which the frequency decreased; thus, the OT-1 T cells were approximately 35% of all CD8$^+$ T cells (Figure 1D). Even out to day 35, however, the CD8$^+$ T-cell compartment consisted of approximately 10% OT-1 cells. In two such experiments, we estimated the absolute number of OT-1 T cells by multiplying the total viable leukocyte count by the percentage of viable cells that were OT-1 T cells. In one experiment, the peak cell number was 1.8×10^6 OT-1 cells at day 20; in the other, it was 2.0×10^6 OT-1 cells at day 15. If we were to assume that all of the input 1×10^4 OT-1 T cells were participating in the local clonal expansion, and that our recovery of liver leukocytes was 100% effective, we would calculate the magnitude of expansion to be approximately 200-fold. However, it is certain that only a subset of the input OT-1 T cells are participating, and that the liver leukocyte recovery is very inefficient. Therefore, all we can say is that the magnitude of clonal expansion in the liver is very much greater than 200-fold. Throughout

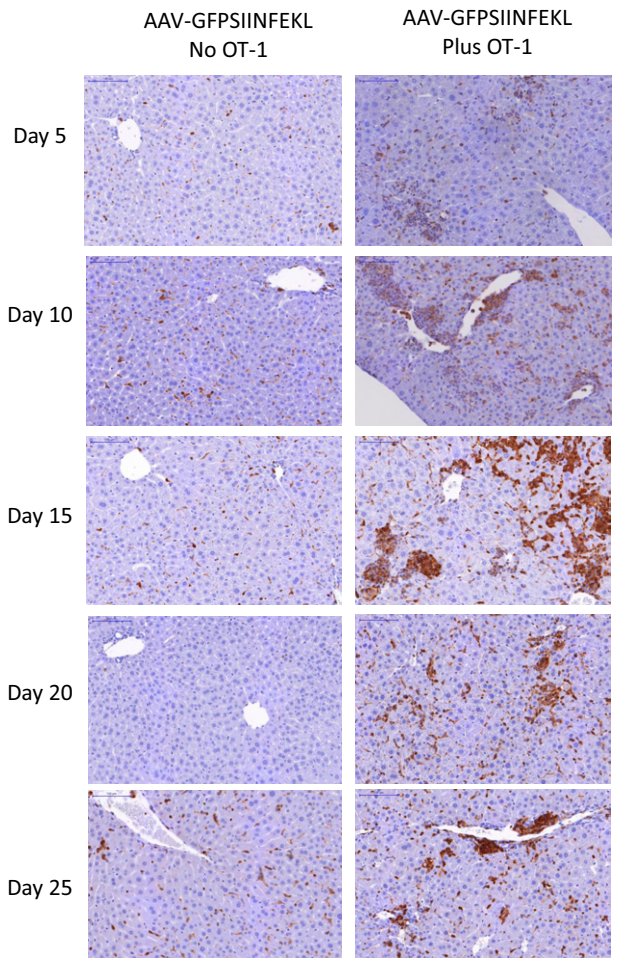

Figure 2. Accumulation of $CD3^+$ cells is highest at day 15 after adoptive transfer. C57BL/6 mice were injected with AAV-GFP-SIINFEKL, followed by no OT-1 $CD8^+$ T cells (**left**) or 1×10^4 OT-1 $CD8^+$ T cells (**right**). Every 5 days thereafter, liver sections were isolated and stained with anti-CD3 antibody. $n = 4$ to 6. Original magnification, ×20.

this time course, OT-1 $CD8^+$ T cells in the spleen and lymph node never exceeded 2.7% and 0.34% of total $CD8^+$ T cells, respectively (data not shown), indicating that the OT-1 $CD8^+$ T cells were activated in the liver, as we have reported previously.[9]

Staining of liver sections with anti-CD3 at various time points after adoptive transfer also showed an increase in $CD3^+$ cells, starting at day 5 and peaking at day 15 (Figure 2). In principle, these cells could be a mixture variously of OT-1 T cells, polyclonal host $CD8^+$ T cells, $CD4^+$ T cells, NK-T cells, or TCR$\gamma\delta$ cells. From flow cytometric analyses (Figure 1, C and D), we can conclude that only a subset (10% to 35%) of the $CD8^+$ T cells were in fact OT-1, and although their numbers argue that the OT-1 cells must have undergone many rounds of cell division, they were still only a minority of the $CD3^+$ cells in the infiltrate.

$CD8^+$ T-cell activation is characterized by the production of the multifunctional cytokine IFNγ (reviewed by Harty et al[16]). Signaling through the IFNγ receptor is necessary for OT-1 $CD8^+$ T-cell-mediated acute liver damage.[12] We therefore looked at expression of IFNγ during the time that OT-1 $CD8^+$ T cells were present in the liver. RNA was harvested from the livers of mice treated with AAV-GFP-SIINFEKL with or without OT-1 T cells every 5 days. Quantitative RT-PCR shows that there was a significant increase in the expression of IFNγ when OT-1 $CD8^+$ T cells were activated in the liver at days 10 and 25 ($P = 0.008$ and $P = 0.014$, respectively) (see Supplemental Figure S1 at *http://ajp.amjpathol.org*). These results show that the activation of OT-1 $CD8^+$ T cells in response to hepatocyte-derived antigen leads to an increase in the expression of IFNγ.

Inefficient Activation of OT-1 $CD8^+$ T Cells in Response to AAV Vector Transgene

Infections of the liver frequently develop into a chronic state in which activation of the $CD8^+$ T cells is suboptimal and not capable of eliminating the pathogen.[17,18] This may be due to the unique environment of the liver and the ability of $CD8^+$ T cells to be activated directly on parenchymal cells in the liver without $CD4^+$ T-cell help.[4] Because of the substantial increase in OT-1 $CD8^+$ T-cell numbers after activation by hepatocellular antigen and in view of the fact that this resulted in increased IFNγ, we next wanted to obtain a more direct representation of the activation state of the OT-1 $CD8^+$ T cells.

Using flow cytometry, we analyzed OT-1 $CD8^+$ T cells for proliferation and activation markers at various time points after the adoptive transfer of 1×10^4 OT-1 T cells. We documented OT-1 $CD8^+$ T-cell division by labeling the T cells with the dye CFSE, but even at early time points the OT-1 $CD8^+$ T cells had diluted the CFSE to background levels, indicating that the cells had undergone at least eight rounds of proliferation.[19] Because of the small number of cells adoptively transferred, it was not possible to use CFSE to visualize earlier proliferation and activation events. The small number of cells also made it impossible to detect the OT-1 $CD8^+$ T cells in a negative control given AAV-GFP without the SIINFEKL peptide. We therefore used host $CD8^+$ T cells from each animal as an internal control for the activated OT-1 $CD8^+$ T cells. The OT-1 cells had high expression of the inhibitory receptor PD-1 up to day 35 after adoptive transfer (Figure 3). These cells were also low in CD62L (the lymph node homing receptor), indicating that they had been activated. With less consistency, we sometimes saw that OT-1 $CD8^+$ T cells had low expression of IL7R-α (CD127). The combination of high PD-1 expression and low CD127 expression is a phenotype characteristic of exhausted $CD8^+$ T cells.[20–22] Given that the OT-1 $CD8^+$ T cells with this phenotype also expressed activation markers, their exact functional status was difficult to interpret.

Increase in Kupffer Cell Numbers after OT-1 $CD8^+$ T-Cell Activation

Kupffer cell prominence is a common phenomenon in chronic hepatitis.[23,24] In light of this feature of hepatitis, we next looked at the presence of Kupffer cells in the liver. F4/80 staining of liver sections from mice treated

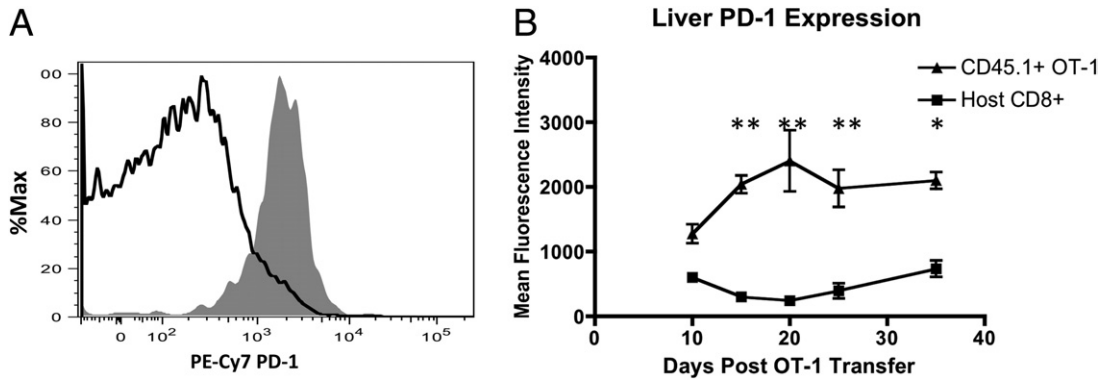

Figure 3. OT-1 CD8$^+$ T cells have high expression of PD-1. C57BL/6 mice were injected with AAV-GFP-SIINFEKL, followed by 1×10^4 OT-1 CD8$^+$ T cells. Liver lymphocytes were harvested every 5 days from day 10 to day 35. PD-1 expression was compared between OT-1 CD8$^+$ T cells and host CD8$^+$ T cells. $^{**}P < 0.02$ (days 15, 20, and 25); $^{*}P = 0.05$ (day 35). The experiment was performed two times; $n = 3$ to 5.

with AAV-GFP-SIINFEKL with or without OT-1 CD8$^+$ T cells showed an increase in Kupffer cells in the presence of antigen-activated OT-1 T cells (Figure 4). Quantitation of this increase shows F4/80 message expression as measured by qRT-PCR (see Supplemental Figure S2 at *http://ajp.amjpathol.org*).

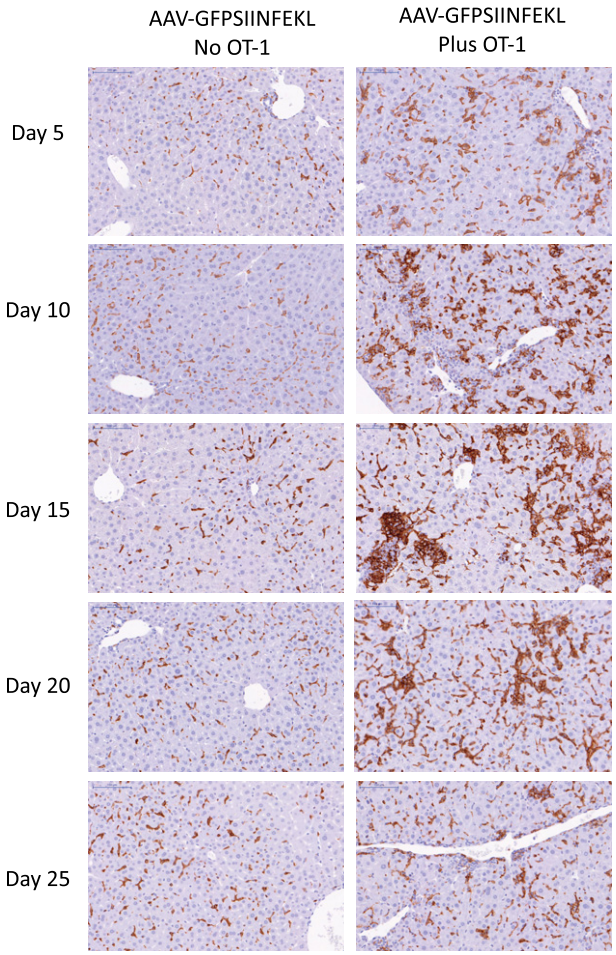

Figure 4. Kupffer cell numbers peak at day 15. C57BL/6 mice were injected with AAV-GFP-SIINFEKL, followed by no OT-1 CD8$^+$ T cells (**left**) or 1×10^4 OT-1 CD8$^+$ T cells (**right**). Livers were harvested every 5 days thereafter and stained for Kupffer cells with anti-F4/80 antibody. $n = 4$ to 6. Original magnification, ×20.

Activation of monocytes by IFNγ leads to increased expression of the chemokines CXCL9 (known also as monokine induced by gamma-IFN, or MIG) and CXCL10 (known also as IFN-induced protein 10, or IP-10), enhancing T-cell recruitment.[12,25–27] Increased levels of both of these chemokines have been found in patients with hepatitis C cirrhotic livers.[28] Because of the increased expression of IFNγ in the livers of AAV-GFP-SIINFEKL-treated mice in the presence of OT-1 CD8$^+$ T cells, we used qRT-PCR to determine whether these chemokines were induced. Mice were treated with vector and then given 1×10^4 OT-1 CD8$^+$ T cells or no OT-1 CD8$^+$ T cells as a control. Both CXCL9 and CXCL10 were up-regulated, both demonstrating the same kinetics of expression (see Supplemental Figure S3, A and B, at *http://ajp.amjpathol.org*). Mice treated with the vector and OT-1 CD8$^+$ T cells showed increased levels of both chemokines at days 5, 10, and 15 (on days 5 and 10, $P < 0.03$, and on day 15, $P < 0.008$; see Supplemental Figure S3 at *http://ajp.amjpathol.org*). Expression of these chemokines was not significantly different on or after day 20. This would be consistent with IFNγ stimulating Kupffer cell activation and the downstream production of chemokines by either these macrophages or liver sinusoidal endothelial cells.

IFNγ is also responsible for the up-regulation of the adhesion molecules, intercellular cell adhesion molecule-1 (ICAM-1) and vascular cell adhesion molecule-1 (VCAM-1).[29,30] These molecules can be expressed on Kupffer cells, liver sinusoidal endothelial cells, and hepatocytes.[31] To gain entry from the blood into an infected tissue, lymphocytes go through a process of tethering to the endothelium, followed by rolling and firm adhesion. Lymphocytes then extravasate through the endothelial layer into the tissue. Tethering and rolling are processes that rely on selectin-addressin interactions, whereas firm adhesion relies on cellular adhesion molecules such as ICAM-1 and VCAM-1 (reviewed by Lee and Kubes[32]). In particular, ICAM-1 is very important in the trapping of activated CD8$^+$ T cells in the liver.[33] To determine whether these adhesion molecules were up-regulated because of OT-1 CD8$^+$ T-cell activation in response to the AAV vector, qRT-PCR was again performed on sam-

ples after adoptive transfer. The expression of both of these molecules was increased significantly at day 15 ($P < 0.008$ for both ICAM-1 and VCAM-1; see Supplemental Figure S3, C and D, at *http://ajp.amjpathol.org*), but not at any other measurement time point.

The increase in Kupffer cell numbers when OT-1 CD8$^+$ T cells were activated, along with the increase in chemokines and adhesion molecules, emphasizes the importance of IFNγ in immunity to hepatocellular antigen. We hypothesize that the activation of Kupffer cells and the ensuing expression of these molecules play a role in the accumulation of OT-1 T cells in the liver between days 10 and 25. In an AAV-based liver injury model in which 5×10^6 OT-1 T cells were administered, resulting in acute self-limiting hepatitis, intracellular staining revealed IFNγ in the T cells. With the present experiments, we cannot definitively say that OT-1 CD8$^+$ T cells are responsible for the production of IFNγ, but we know that their recognition of antigen in the liver leads to an increase in the numbers of Kupffer cells and the up-regulation of IFNγ-responsive genes.

Administration of OT-1 CD8$^+$ T Cells Does Not Result in Elimination of the AAV Vector DNA but Does Result in a Significant Decrease in AAV Vector RNA

Despite the expression of some markers of exhaustion, activation of OT-1 CD8$^+$ T cells by hepatocellular antigen leads to IFNγ production, an increase in Kupffer cell numbers, and the expression of molecules that augment T-cell recruitment. In light of these contradictory findings, we next determined the effect of OT-1 CD8$^+$ T cells on the vector itself. Again, C57BL/6 mice were injected with AAV-GFP-SIINFEKL, followed 3 weeks later by adoptive transfer of 1×10^4 OT-1 CD8$^+$ T cells. Seven separate experiments were done, in which livers were harvested at day 35 after adoptive transfer, followed by purification of RNA and DNA. This late time point allowed us to determine the long-term effects of OT-1 T-cell activation, after their numbers had declined. We used qPCR to determine the presence or absence of vector DNA as measured by eGFP (Figure 5A) and used qRT-PCR to determine expression of vector RNA, also measured by eGFP (Figure 5B). These overall results show that OT-1 cells were not able to eliminate vector-transduced hepatocytes but did cause a significant decrease ($P < 0.0001$, two-way analysis of variance across all experiments) in expression of vector. Nonetheless, these experiments yielded varied outcomes. In one case there was no effect on the level of vector RNA; in several there was a twofold effect, and in others up to a 10-fold effect.

Effect of CD8$^+$ T-Cell Response on Vector RNA Expression and Hepatitis

To examine the relationship between OT-1 T cells, time of assay, liver injury, and the suppression of vector expression, we performed time-course analyses lasting up to 45 days. Two similar experiments had different outcomes. In one experiment (Figure 6, A, C, and E), q-PCR used to measure the abundance of OT-1 T cells showed a brief peak at day 10 (Figure 6A), followed by a 10-fold reduction in signal by day 15. In this experiment, the suppression of vector RNA expression was unusually strong (>10-fold), clear already on day 10 and sustained thereafter (Figure 6C). This was accompanied by acute hepatitis with elevated ALT on day 10, returning thereafter to normal (Figure 6E). Another experiment (Figure 6, B, D, and F), which we performed in exactly the same way, yielded contrasting results, with a slower increase in OT-1 T-cell abundance (Figure 6B), no clear effect on the level of vector RNA expression (Figure 6D), and a chronic course in which ALT was significantly elevated on day 15 and again on day 25 (Figure 6F). These data are consistent with a model in which the initial course of the expansion of these relatively low numbers of OT-1 T cells is to some extent stochastic, but it determines the severity and duration of hepatitis and the efficiency of the T-cell response in suppressing vector expression. The slower-burning hepatitis experiment also revealed sustained abundance of CD3$^+$ T cells and Kupffer cells by immunohistology (Figures 2 and 4), as well as fibrogenesis (discussed below).

The primers we used for the detection of vector-derived eGFP did not span exon boundaries, so we could

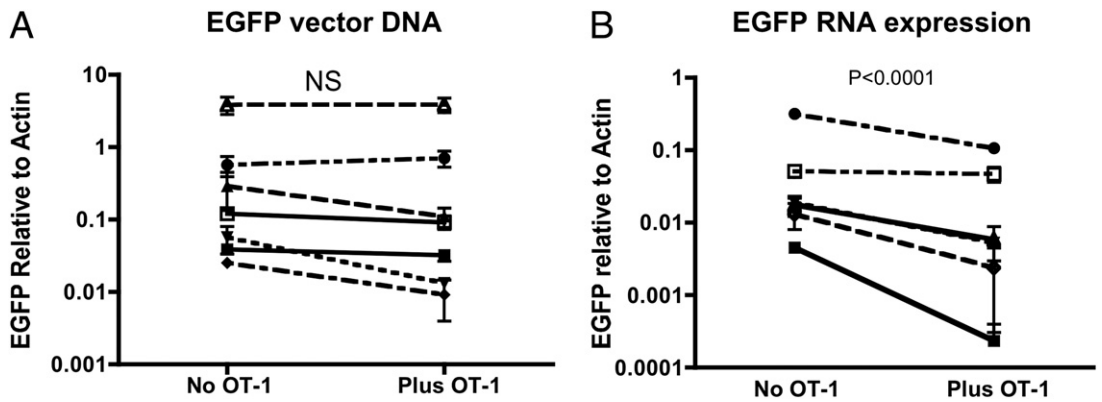

Figure 5. OT-1 CD8$^+$ T cells caused decreased vector RNA but not decreased vector DNA. C57BL/6 mice were injected with AAV-GFP-SIINFEKL, followed by no OT-1 CD8$^+$ T cells or 1×10^4 OT-1 CD8$^+$ T cells. Seven experiments were harvested on day 35 after adoptive transfer and analyzed by qPCR for DNA (**A**) and by qRT-PCR for RNA (**B**). Each symbol represents one experiment. Two-way analysis of variance. $n = 38$ (No OT-1); $n = 32$ (Plus OT-1).

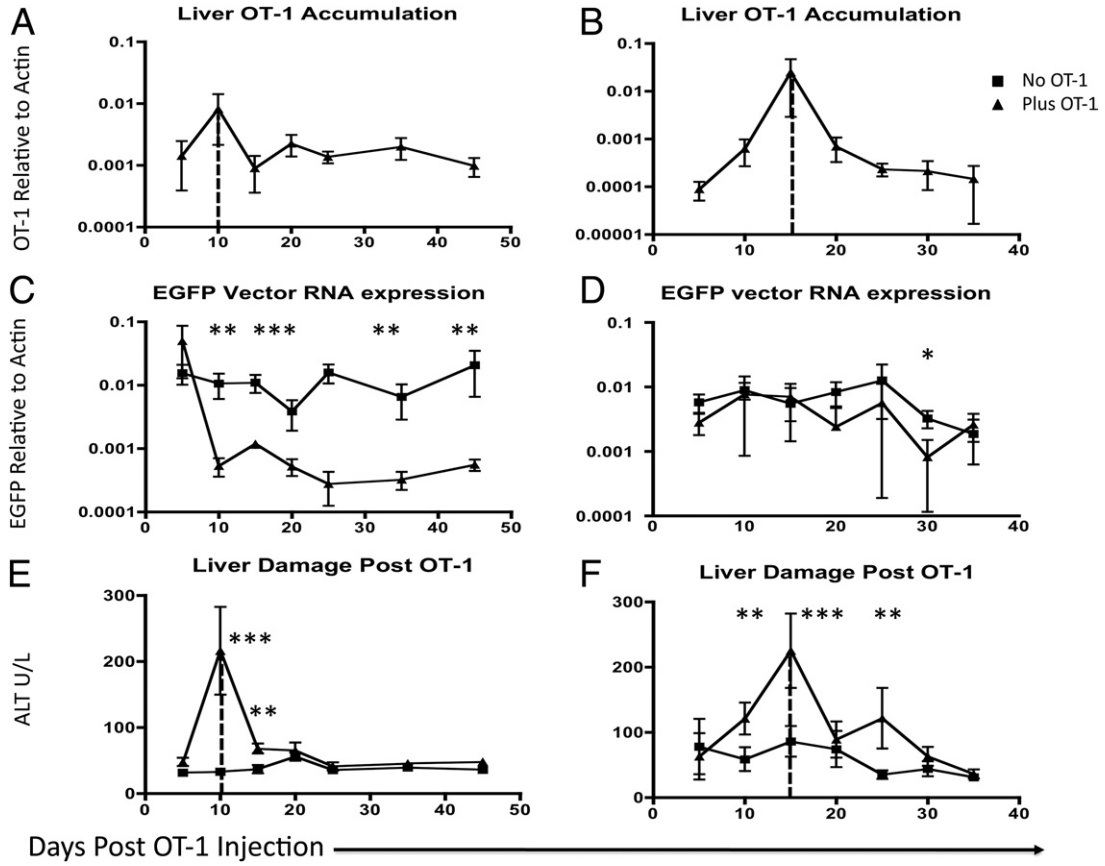

Figure 6. The nature of the OT-1 CD8$^+$ T-cell response dictates vector RNA elimination and liver damage. C57BL/6 mice were injected with AAV-GFP-SIINFEKL, followed by no OT-1 CD8$^+$ T cells or by 1×10^4 OT-1 CD8$^+$ T cells. Every 5 days thereafter, livers were harvested. **A** and **B:** OT-1 cell accumulation as measured by qPCR. **C** and **D:** Vector RNA expression as measured by qRT-PCR. **E** and **F:** Liver damage as measured by serum ALT. Each plot represents 3 to 6 mice. The two experiments, performed in exactly the same way, yielded different outcomes (**A**, **C**, and **E** versus **B**, **D**, and **F**). The dashed lines in **A**, **B**, **E**, and **F** represent the peaks in OT-1 numbers and ALT values. $^{**}P < 0.03$ (days 10, 35, and 45) and $^{***}P < 0.008$ (day 15 (**C**); $^{*}P = 0.05$ (day 30) (**D**); $^{**}P < 0.03$ on day 15 and $^{***}P < 0.008$ (day 10) (**E**); $^{**}P < 0.03$ (days 10 and 25) and $^{***}P < 0.008$ (day 15) (**F**). The data did not reach significance at any other time point.

use the same primers both for genomic DNA and for cDNA amplification. Although the TRIzol extraction would be expected to purify RNA, it is true that if this extraction was flawed, some DNA could have contaminated the cDNA, resulting in unwanted assay background. We therefore repeated the qRT-PCR analysis of vector expression in one of the experiments shown in Figure 6, after DNase treatment of the isolated RNA. The outcome was essentially the same. For the two data sets presented side by side, see Supplemental Figure S4 (available at *http://ajp.amjpathol.org*).

The ALT findings were supported by H&E staining of liver sections at various time points after OT-1 T-cell injection (Figure 7) for the chronic course of hepatitis. Inflammatory infiltrates and Councilman bodies (areas of pink, glassy staining representing apoptotic hepatocytes) were detected at all time points tested when OT-1 CD8$^+$ T cells were administered, but not in their absence. Hepatitis was most robust at day 15, however, confirming the ALT results. The similar curves for both the accumulation of OT-1 CD8$^+$ T cells and the increase in ALT levels suggests that the OT-1 CD8$^+$ T cells were activated and caused long-term immunopathology.

OT-1 T-Cell Response to Vector Leads to Stellate Cell Activation and Fibrogenesis

A common outcome of chronic hepatitis is fibrosis, a serious clinical problem that often leads to cirrhosis and to hepatocellular carcinoma. Fibrosis results from the deposition of collagen by activated stellate cells and occurs in an attempt to repair the damaged tissue (reviewed by Brenner[34]). Because hepatitis was sustained when 1×10^4 OT-1 CD8$^+$ T cells were slower to accumulate in response to AAV-GFP-SIINFEKL injection in mice, we stained liver tissue to detect stellate cell activation and the deposition of fibrous tissue. Stellate cell activation was detected by staining for SMA (Figure 8). When mice were treated with AAV-GFP-SIINFEKL but not OT-1 T cells, very little SMA staining was found. In the presence of vector and OT-1 CD8$^+$ T cells, however, an increase in SMA was seen on day 15 (at the peak of inflammation and OT-1 CD8$^+$ T-cell infiltration). Stellate cell activation was coincident with an increase in the generation of fibrosis as measured by Sirius Red staining (Figure 9). This was seen in mice that received OT-1 CD8$^+$ T cells, but not in untreated mice, and was most prominent at day 15. After day 15, the Sirius Red staining decreased, indicating that in this

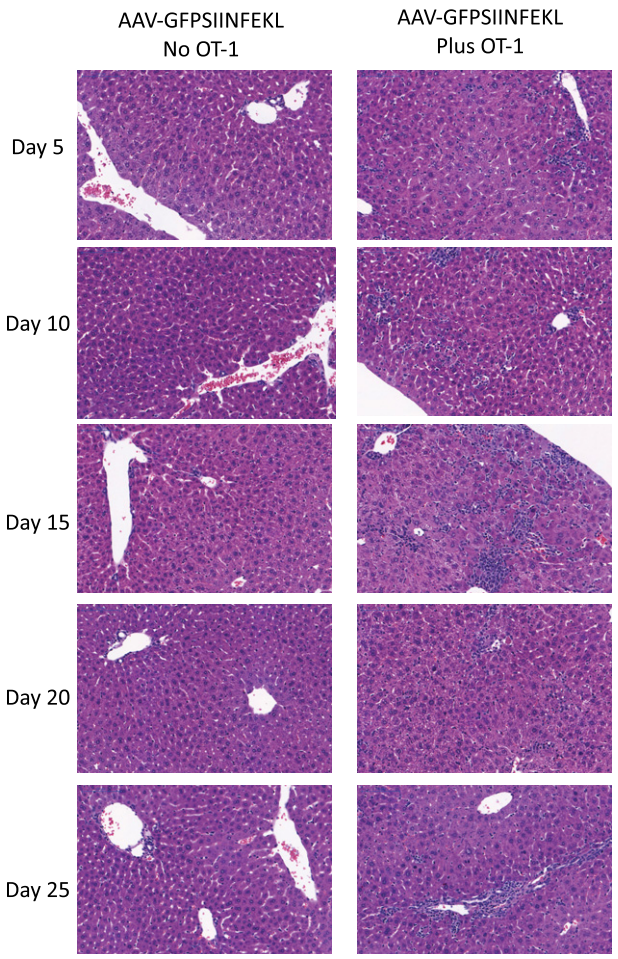

Figure 7. OT-1 CD8$^+$ T cells cause long-term liver damage as evidenced by H&E staining. C57BL/6 mice were injected with AAV-GFP-SIINFEKL, followed by no OT-1 CD8$^+$ T cells (**left**) or 1 × 10^4 OT-1 CD8$^+$ T cells (**right**). Livers were harvested every 5 days and stained with H&E. Images are from an experiment that exhibited chronic inflammation. n = 4 to 6. Original magnification, ×20.

experimental model fibrosis also diminished. Importantly, the generation of fibrosis and activation of stellate cells in this chronic model of hepatitis is not seen in the more acute model used in our lab previously.[12] These events were also absent when a more robust CD8$^+$ T-cell response was initiated, presumably because of the abbreviated liver damage (Figure 6, A, C, and E).

Discussion

The administration of the AAV-GFP-SIINFEKL vector followed by 1 × 10^4 OT-1 T cells provides a mouse model (one of only a few) in which it is possible to document long-term immune-mediated liver damage and fibrosis. Similar to chronic liver infections in humans, the administration of 1 × 10^4 OT-1 CD8$^+$ T cells after AAV-GFP-SIINFEKL administration resulted in the slow accumulation of these cells in the liver, accompanied by prolonged damage. With the establishment of a model that more closely represents an endogenous CD8$^+$ T-cell response to hepatocyte-derived antigen, we wanted to determine the activation state of the CD8$^+$ T cells and what their effect was on the vector itself.

By two different methods, we showed that OT-1 CD8$^+$ T-cell numbers peak at approximately day 15 and gradually decrease thereafter. These cells were activated, as measured by down-regulation of CD62L (data not shown). The activation of OT-1 CD8$^+$ T cells was coincident with an increase in Kupffer cells and an increase in IFNγ and IFNγ-responsive genes. However, the OT-1 CD8$^+$ T cells also had very high PD-1 expression and (less consistently) low CD127 expression consistent with an exhausted phenotype. An exhausted state is characterized by CD8$^+$ T cells that have the phenotype of PD-1^{hi} and CD127^{lo}.[22] PD-1 is a suppressive molecule, whereas CD127 is the receptor for IL-7. CD127 is typically up-regulated to promote T-cell survival in memory cells. Exhausted cells also are deficient in their ability to make the effector cytokines IL-2 and IFNγ, a deficiency thought to result from constant exposure to antigen.[35] Perhaps because of high PD-1 expression, the OT-1 CD8$^+$ T cells were not able to eliminate the vector from the liver; they were, however, capable of causing decreased expression of RNA.

Our observation of decreased vector RNA expression but no effect on vector DNA could be attributed to two different mechanisms. One possibility is that RNA is directly suppressed by the anti-viral cytokine IFNγ, similar

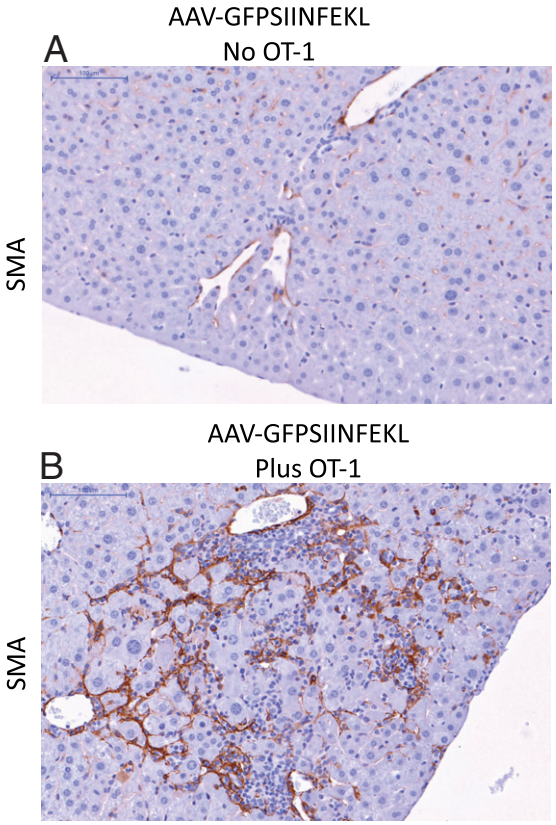

Figure 8. OT-1 CD8$^+$ T-cell activation causes downstream activation of hepatic stellate cells. C57BL/6 mice were injected with AAV-GFPS-SIINFEKL, followed by no OT-1 CD8$^+$ T cells (**left**) or 1 × 10^4 OT-1 CD8$^+$ T cells (**right**). Livers were harvested at day 15 after adoptive transfer and stained for SMA. Images are from an experiment that exhibited chronic inflammation. n = 4 to 6. Original magnification, ×20.

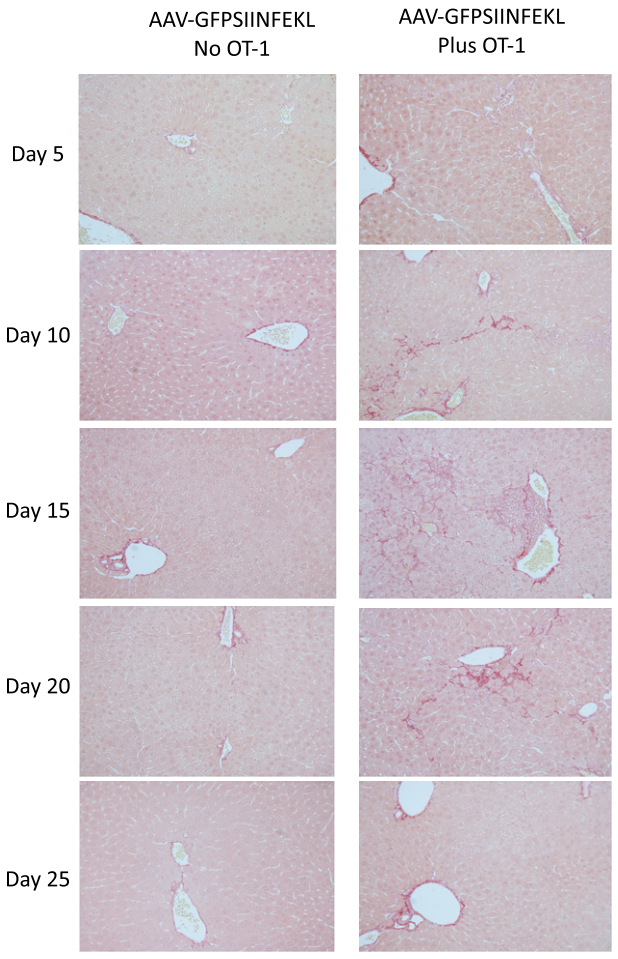

Figure 9. OT-1 $CD8^+$ T-cell activation leads to fibrogenesis. C57BL/6 mice were injected with AAV-GFP-SIINFEKL, followed by no OT-1 $CD8^+$ T cells (**left**) or 1×10^4 OT-1 $CD8^+$ T cells (**right**). Every 5 days, livers were harvested and stained with Sirius Red. Images are from an experiment that exhibited chronic inflammation. $n = 4$ to 6. Original magnification, ×20.

to what happens in an HBV transgenic mouse.[7] The second possibility is that a large number of hepatocytes are transduced, but only a subset of those cells express the majority of vector RNA. If OT-1 $CD8^+$ T cells eliminated these high expressors, PCR would reveal a significant effect on vector RNA but none on vector DNA, as we observed with the present model.

Activation of OT-1 $CD8^+$ T cells elicited liver damage, the duration of which was dependent on the strength of the initial T-cell response and consequently on the ability of those cells to eliminate vector expression. These findings are in line with findings in human HCV patients, who generate a robust $CD8^+$ T-cell response and resolve the viral infection as well as the hepatitis. Those who do not have a robust $CD8^+$ T-cell response do not eliminate the virus and have chronic surges of hepatitis.[36] In the time course in which vector expression was not eliminated and inflammation persisted, we also saw fluctuation in liver damage, whereby hepatitis seemed to be resolved at day 20 but returned on day 25. Furthermore, in the absence of this prolonged hepatitis, fibrogenesis did not occur, and stellate cell activation was minimal (data not shown).

Despite hepatitis in both cases, AAV vector DNA was not effected by the activation of OT-1 $CD8^+$ T cells. This might suggest that the majority of the liver injury was an example of collateral damage,[37] also known as bystander hepatitis.[38] The resolution of hepatitis was dependent on the presence of vector RNA expression (Figure 6). In the context of a robust OT-1 $CD8^+$ T-cell response, vector RNA expression was diminished, corresponding with decreased hepatitis. If the OT-1 $CD8^+$ T-cell response was slower to accumulate, however, vector RNA expression was sustained and hepatitis persisted.

The increase in Kupffer cell numbers was dramatic in the presence of OT-1 T-cell activation. These cells are strongly activated by IFNγ, which may have been produced by the activated OT-1 $CD8^+$ T cells.[39] IFNγ likely played a role in the increase in chemokines and adhesion molecules from day 5 to day 15. The increase in these molecules could be important in the recruitment,[40] retention,[33,41] and activation[41] of the OT-1 T cells in the liver.

The increase in $CD8^+$ T cells and in IFNγ-responsive genes was also coincident with elevated liver enzymes. In an investigation of immunopathology induced by the acute response of a much larger number of T cells to AAV-endcoded hepatocellular antigen, Giannandrea et al[12] showed that this cytokine is important in the liver damage. The damage caused was due to both an indirect mechanism, whereby IFNγ-activated Kupffer cells produce TNFα, and a direct mechanism, whereby IFNγ directly injured the liver parenchyma. Neither of these mechanisms, however, is specific to killing of vector-transduced hepatocytes; nonspecific antigen-independent killing of hepatocytes has also been seen in mice infected with influenza, due to the trapping of activated $CD8^+$ T cells in the liver.[42] It is possible that, in the present experiments, nonspecific hepatocyte death occurred in consequence of the increase in IFNγ, among other factors. This would account for the presence of hepatitis but the absence of vector elimination.

The generation of fibrosis seen in the present study is unique among models of immune-mediated hepatitis in mice. Because most mouse models of hepatitis are more acute in nature, including the previous model published by our lab,[12] the generation of fibrosis does not occur. In the present model, fibrogenesis increases with T-cell numbers and liver damage and recedes in a similar manner, although not to complete resolution. A mouse model using carbon tetrachloride to induce fibrosis has shown that the expression of matrix metalloproteinases by bone marrow-derived cells contributes to the regression of fibrosis.[43] In the context of treatments such as lamivudine (for HBV) and interferon therapy (for HCV), reversal of fibrosis can occur in humans.[44–48] The regression of fibrosis seen with our present model is confirmed by the fact that hepatic stellate cells (the cells responsible for collagen deposition) were most activated on day 15, but were found in reduced numbers thereafter. In the rodent, regression of fibrosis is associated with the apoptosis of activated stellate cells.[49] This would be consistent with both the decrease in fibrosis and activated stellate cells seen in the present model.

The model we have described here has several features that mimic chronic hepatitis in humans. First, as in HCV and HBV, activation of $CD8^+$ T cells leads to high

expression of PD-1.[50,51] Second, an increase in Kupffer cells is seen in both the present experiments and in chronic liver infections.[52] The expression of CXCL9 and CXCL10 is also up-regulated in HCV infections.[1–3,28,53] The activation of Kupffer cells and the consequent recruitment of $CD8^+$ T cells are likely important in the ensuing long-term liver damage seen in both the present study and in human cases. However, this immune response is inefficient at eliminating vector transduced hepatocytes, similar to the immune failure observed in most cases of chronic HCV.[54] The $CD8^+$ T cells are able to eliminate vector RNA; as in humans, the extent of elimination is more complete in the context of a more robust immune response. This is similar to what is observed in human patients who generate vigorous $CD8^+$ T-cell responses and have acute HCV with resolution, compared with those who have weaker responses and develop chronic HCV.[55] Finally, the inflammation that occurs in response to $CD8^+$ T-cell activation leads to the activation of hepatic stellate cells and the generation of fibrosis, an occurrence commonly seen in humans.

In thinking of this system as a model of human hepatitis, it is important to acknowledge the fact that the $CD8^+$ T cells used in the present study are specific to only one epitope of the ovalbumin protein, SIINFEKL. In human disease, it is unlikely that $CD8^+$ T cells are specific to only one epitope; however, patients who generate chronic disease are usually those with a much more restricted $CD8^+$ T-cell response.[56] These features establish the AAV model outlined here as a useful tool for study of immune-mediated processes that lead to hepatitis and fibrosis in humans.

Acknowledgments

We thank Dr. K. Reed Clarke for the preparation of the AAV vectors and Patricia A. Bourne for excellent immunohistochemistry services.

References

1. Bertolino P, Bowen DG, McCaughan GW, Fazekas de St Groth B: Antigen-specific primary activation of CD8+ T cells within the liver. J Immunol 2001, 166:5430–5438
2. Lee YC, Lu L, Fu F, Li W, Thomson AW, Fung JJ, Qian S: Hepatocytes and liver nonparenchymal cells induce apoptosis in activated T cells. Transplant Proc 1999, 31:784
3. Bertolino P, Trescol-Biemont MC, Rabourdin-Combe C: Hepatocytes induce functional activation of naive CD8+ T lymphocytes but fail to promote survival. Eur J Immunol 1998, 28:221–236
4. Wuensch SA, Spahn J, Crispe IN: Direct, help-independent priming of CD8+ T cells by adeno-associated virus-transduced hepatocytes. Hepatology 2010, 52:1068–1077
5. Sass G, Heinlein S, Agli A, Bang R, Schumann J, Tiegs G: Cytokine expression in three mouse models of experimental hepatitis. Cytokine 2002, 19:115–120
6. Tiegs G, Hentschel J, Wendel A: A T cell-dependent experimental liver injury in mice inducible by concanavalin A. J Clin Invest 1992, 90:196–203
7. G Guidotti LG, Ishikawa T, Hobbs MV, Matzke B, Schreiber R, Chisari FV: Intracellular inactivation of the hepatitis B virus by cytotoxic T lymphocytes. Immunity 1996, 4:25–36
8. Zinkernagel RM, Haenseler E, Leist T, Cerny A, Hengartner H, Althage A: T cell-mediated hepatitis in mice infected with lymphocytic choriomeningitis virus. Liver cell destruction by H-2 class I-restricted virus-specific cytotoxic T cells as a physiological correlate of the 51Cr-release assay? J Exp Med 1986, 164:1075–1092
9. Wuensch SA, Pierce RH, Crispe IN: Local intrahepatic CD8+ T cell activation by a non-self-antigen results in full functional differentiation. J Immunol 2006, 177:1689–1697
10. Snyder RO, Miao CH, Patijn GA, Spratt SK, Danos O, Nagy D, Gown AM, Winther B, Meuse L, Cohen LK, Thompson AR, Kay MA: Persistent and therapeutic concentrations of human factor IX in mice after hepatic gene transfer of recombinant AAV vectors. Nat Genet 1997, 16:270–276
11. Gosálvez J, Rodríguez-Iñigo E, Ramiro-Díaz JL, Bartolomé J, Tomás JF, Oliva H, Carreño V: Relative quantification and mapping of hepatitis C virus by in situ hybridization and digital image analysis. Hepatology 1998, 27:1428–1434
12. Giannandrea M, Pierce RH, Crispe IN: Indirect action of tumor necrosis factor-alpha in liver injury during the CD8+ T cell response to an adeno-associated virus vector in mice. Hepatology 2009, 49:2010–2020
13. Hogquist KA, Jameson SC, Heath WR, Howard JL, Bevan MJ, Carbone FR: T cell receptor antagonist peptides induce positive selection. Cell 1994, 76:17–27
14. Badovinac VP, Haring JS, Harty JT: Initial T cell receptor transgenic cell precursor frequency dictates critical aspects of the CD8(+) T cell response to infection. Immunity 2007, 26:827–841
15. Azadniv M, Dugger K, Bowers WJ, Weaver C, Crispe IN: Imaging CD8+ T cell dynamics in vivo using a transgenic luciferase reporter. Int Immunol 2007, 19:1165–1173
16. Harty JT, Tvinnereim AR, White DW: CD8+ T cell effector mechanisms in resistance to infection. Annu Rev Immunol 2000, 18:275–308
17. Spangenberg HC, Viazov S, Kersting N, Neumann-Haefelin C, McKinney D, Roggendorf M, von Weizsäcker F, Blum HE, Thimme R: Intrahepatic CD8+ T-cell failure during chronic hepatitis C virus infection. Hepatology 2005, 42:828–837
18. Gruener NH, Lechner F, Jung MC, Diepolder H, Gerlach T, Lauer G, Walker B, Sullivan J, Phillips R, Pape GR, Klenerman P: Sustained dysfunction of antiviral CD8+ T lymphocytes after infection with hepatitis C virus. J Virol 2001, 75:5550–5558
19. Hodgkin PD, Lee JH, Lyons AB: B cell differentiation and isotype switching is related to division cycle number. J Exp Med 1996, 184:277–281
20. Urbani S, B Amadei, D Tola, M Massari, S Schivazappa, G Missale, C Ferrari: PD-1 expression in acute hepatitis C (HCV) invection is associated with HCV-specific CD8+ exhaustion. J Virol 2006, 80:11398–11403
21. Bengsch B, Spangenberg HC, Kersting N, Neumann-Haefelin C, Panther E, von Weizsäcker F, Blum HE, Pircher H, Thimme R: Analysis of CD127 and KLRG1 expression on hepatitis C virus-specific CD8+ T cells reveals the existence of different memory T-cell subsets in the peripheral blood and liver. J Virol 2007, 81:945–953
22. Radziewicz H, Ibegbu CC, Fernandez ML, Workowski KA, Obideen K, Wehbi M, Hanson HL, Steinberg JP, Masopust D, Wherry EJ, Altman JD, Rouse BT, Freeman GJ, Ahmed R, Grakoui A: Liver-infiltrating lymphocytes in chronic human hepatitis C virus infection display an exhausted phenotype with high levels of PD-1 and low levels of CD127 expression. J Virol 2007, 81:2545–2553
23. Roberts JM, Searle JW, Cooksley WG: Histological patterns of prolonged hepatitis C infection. Gastroenterol Jpn 1993, 28 Suppl 5:37–41
24. Bach N, Thung SN, Schaffner F: The histological features of chronic hepatitis C and autoimmune chronic hepatitis: a comparative analysis. Hepatology 1992, 15:572–577
25. Liao F, Rabin RL, Yannelli JR, Koniaris LG, Vanguri P, Farber JM: Human Mig chemokine: biochemical and functional characterization. J Exp Med 1995, 182:1301–1314
26. Luster AD, Unkeless JC, Ravetch JV: Gamma-interferon transcriptionally regulates an early-response gene containing homology to platelet proteins. Nature 1985, 315:672–676
27. Taub DD, Lloyd AR, Conlon K, Wang JM, Ortaldo JR, Harada A, Matsushima K, Kelvin DJ, Oppenheim JJ: Recombinant human interferon-inducible protein 10 is a chemoattractant for human monocytes and T lymphocytes and promotes T cell adhesion to endothelial cells. J Exp Med 1993, 177:1809–1814
28. Shields PL, Morland CM, Salmon M, Qin S, Hubscher SG, Adams DH: Chemokine and chemokine receptor interactions provide a mechanism for selective T cell recruitment to specific liver compartments within hepatitis C-infected liver. J Immunol 1999, 163:6236–6243

29. Hughes C, Male DK, Lantos PL: Adhesion of lymphocytes to cerebral microvascular cells: effects of interferon-gamma, tumour necrosis factor and interleukin-1. Immunology 1988, 64:677–681
30. Look DC, Pelletier MR, Holtzman MJ: Selective interaction of a subset of interferon-gamma response element-binding proteins with the intercellular adhesion molecule-1 (ICAM-1) gene promoter controls the pattern of expression on epithelial cells. J Biol Chem 1994, 269:8952–8958
31. Dillon P, Belchis D, Tracy T, Cilley R, Hafer L, Krummel T: Increased expression of intercellular adhesion molecules in biliary atresia. Am J Pathol 1994, 145:263–267
32. Lee WY, Kubes P: Leukocyte adhesion in the liver: distinct adhesion paradigm from other organs. J Hepatol 2008, 48:504–512
33. John B, Crispe IN: Passive and active mechanisms trap activated CD8+ T cells in the liver. J Immunol 2004, 172:5222–5229
34. Brenner DA: Molecular pathogenesis of liver fibrosis. Trans Am Clin Climatol Assoc 2009, 120:361–368
35. Wherry EJ, Blattman JN, Murali-Krishna K, van der Most R, Ahmed R: Viral persistence alters CD8 T-cell immunodominance and tissue distribution and results in distinct stages of functional impairment. J Virol 2003, 77:4911–4927
36. Rehermann B: Hepatitis C virus versus innate and adaptive immune responses: a tale of coevolution and coexistence. J Clin Invest 2009, 119:1745–1754
37. Mehal WZ, Azzaroli F, Crispe IN: Antigen presentation by liver cells controls intrahepatic T cell trapping, whereas bone marrow-derived cells preferentially promote intrahepatic T cell apoptosis. J Immunol 2001, 167:667–673
38. Bowen DG, Warren A, Davis T, Hoffmann MW, McCaughan GW, Fazekas de St Groth B, Bertolino P: Cytokine-dependent bystander hepatitis due to intrahepatic murine CD8 T-cell activation by bone marrow-derived cells. Gastroenterology 2002, 123:1252–1264
39. Perussia B, Dayton ET, Fanning V, Thiagarajan P, Hoxie J, Trinchieri G: Immune interferon and leukocyte-conditioned medium induce normal and leukemic myeloid cells to differentiate along the monocytic pathway. J Exp Med 1983, 158:2058–2080
40. Hokeness KL, Deweerd ES, Munks MW, Lewis CA, Gladue RP, Salazar-Mather TP: CXCR3-dependent recruitment of antigen-specific T lymphocytes to the liver during murine cytomegalovirus infection. J Virol 2007, 81:1241–1250
41. Bertolino P, Arnhild Schrage, David G. Bowen, Katja Kl Bertolino P, Schrage A, Bowen DG, Klugewitz K, Ghani S, Eulenburg K, Holz L, Hogg N, McCaughan GW, Hamann A: Early intrahepatic antigen-specific retention of naive CD8+ T cells is predominantly ICAM-1/LFA-1 dependent in mice. Hepatology 2005, 42:1063–1071
42. Polakos NK, Cornejo JC, Murray DA, Wright KO, Treanor JJ, Crispe IN, Topham DJ, Pierce RH: Kupffer cell-dependent hepatitis occurs during influenza infection. Am J Pathol 2006, 168:1169–1178; quiz 1404–1165
43. Higashiyama R, Inagaki Y, Hong YY, Kushida M, Nakao S, Niioka M, Watanabe T, Okano H, Matsuzaki Y, Shiota G, Okazaki I: Bone marrow-derived cells express matrix metalloproteinases and contribute to regression of liver fibrosis in mice. Hepatology 2007, 45:213–222
44. Kweon YO, Goodman ZD, Dienstag JL, Schiff ER, Brown NA, Burchardt E, Schoonhoven R, Brenner DA, Fried MW: Decreasing fibrogenesis: an immunohistochemical study of paired liver biopsies following lamivudine therapy for chronic hepatitis B. J Hepatol 2001, 35:749–755
45. Dienstag JL, Goldin RD, Heathcote EJ, Hann HW, Woessner M, Stephenson SL, Gardner S, Gray DF, Schiff ER: Histological outcome during long-term lamivudine therapy. Gastroenterology 2003, 124:105–117
46. Shiratori Y, Imazeki F, Moriyama M, Yano M, Arakawa Y, Yokosuka O, Kuroki T, Nishiguchi S, Sata M, Yamada G, Fujiyama S, Yoshida H, Omata M: Histologic improvement of fibrosis in patients with hepatitis C who have sustained response to interferon therapy. Ann Intern Med 2000, 132:517–524
47. Poynard T, McHutchison J, Manns M, Trepo C, Lindsay K, Goodman Z, Ling MH, Albrecht J: Impact of pegylated interferon alfa-2b and ribavirin on liver fibrosis in patients with chronic hepatitis C. Gastroenterology 2002, 122:1303–1313
48. Farci P, Roskams T, Chessa L, Peddis G, Mazzoleni AP, Scioscia R, Serra G, Lai ME, Loy M, Caruso L, Desmet V, Purcell RH, Balestrieri A: Long-term benefit of interferon alpha therapy of chronic hepatitis D: regression of advanced hepatic fibrosis. Gastroenterology 2004, 126:1740–1749
49. Iredale JP, Benyon RC, Pickering J, McCullen M, Northrop M, Pawley S, Hovell C, Arthur MJ: Mechanisms of spontaneous resolution of rat liver fibrosis. Hepatic stellate cell apoptosis and reduced hepatic expression of metalloproteinase inhibitors. J Clin Invest 1998, 102:538–549
50. Larrubia JR, Benito-Martínez S, Miquel J, Calvino M, Sanz-de-Villalobos E, Parra-Cid T: Costimulatory molecule programmed death-1 in the cytotoxic response during chronic hepatitis C. World J Gastroenterol 2009, 15:5129–5140
51. Liang XS, Zhou Y, Li CZ, Wan MB: Natural course of chronic hepatitis B is characterized by changing patterns of programmed death type-1 of CD8-positive T cells. World J Gastroenterol 2010, 16:618–624
52. Dolganiuc A, Norkina O, Kodys K, Catalano D, Bakis G, Marshall C, Mandrekar P, Szabo G: Viral and host factors induce macrophage activation and loss of toll-like receptor tolerance in chronic HCV infection. Gastroenterology 2007, 133:1627–1636
53. Helbig KJ, Ruszkiewicz A, Lanford RE, Berzsenyi MD, Harley HA, McColl SR, Beard MR: Differential expression of the CXCR3 ligands in chronic hepatitis C virus (HCV) infection and their modulation by HCV in vitro. J Virol 2009, 83:836–846
54. Boonstra A, van der Laan LJ, Vanwolleghem T, Janssen HL: Experimental models for hepatitis C viral infection. Hepatology 2009, 50:1646–1655
55. Neumann-Haefelin C, Hans Christian Spangenberg, Hubert E Blum, and Robert Thimme: Host and viral factors contributing to CD8+ T cell failure in hepatitis C virus infection. World J Gastroenterol 2007, 13:4839–4847
56. Gruner NH, Gerlach TJ, Jung MC, Diepolder HM, Schirren CA, Schraut WW, Hoffmann R, Zachoval R, Santantonio T, Cucchiarini M, Cerny A, Pape GR: Association of hepatitis C virus-specific CD8+ T cells with viral clearance in acute hepatitis C. J Infect Dis 2000, 181:1528–1536